La Metallurgia Italiana
International Journal of the Italian Association for Metallurgy

Comparison between high-pressure die-cast and rheo-cast aluminium-SICp MMC; wear and friction behaviour

A. E. W. Jarfors, R. Ghasemi, S. Awe, C. K. Jammula

Aluminium is essential in automobile industry together with cast iron. Because of its lightweight property and good mechanical properties, aluminium reinforced with silicon carbide have found application as brake discs. Aluminium reinforced with 15% and 20% silicon carbide were high-pressure die-cast (HPDC) and Rheo-HPDC cast in the current paper. Micro-Vickers hardness and Rockwell C hardness showed different trends with the increasing amounts of SiCp-particles. Scratch resistance of the surface on micro-scale was analysed using a micro-scratch test to study the mechanics of the wear process. Reciprocating sliding wear of the composites was considered, using the HPDC cast aluminium with 20% silicon carbide of liquid casting as the sliding surface. The wear showed a combination of abrasive wear and adhesive wear. The metallography of the wear surfaces showed deep abrasive wear grooves. Wear debris from both the surfaces were forming a tribolayer. The formation of this layer decided the friction and wear performance as a result of the abrasive and adhesive wear mechanisms seen both in the micromechanics of the scratch test and in the friction behaviour.

KEYWORDS: ALUMINIUM, METAL MATRIX COMPOSITE, HIGH-PRESSURE DIE-CASTING, RHEOCASTING, WEAR

BACKGROUND

The need for lightweight solution for moving parts in transport solutions increases as requirements on energy efficiency and carbon footprint are increasing. Weight reduction is vital for carbon footprint reduction. (1) Brake disc rotors is an example of a critical component targeted for weight reduction. (2). Aluminium MMC brake rotors are fabricated using stir casting. (3) Al-SiCp MMCs commonly used requires that Si is present as an alloying element to stabilize the SiCp particles. (2) As a consequence, the Al-SiCp has a matrix that is nearly eutectic, even though other examples exists. (3). In the current study, the friction and wear performance was investigated for two levels of SiCp additions (15 and 20%) fabricated by stir casting and subsequently cast. The casting process studied were conventional high-pressure die-casting and rheocasting. The aim was here to better understand the wear and friction performance by modifying the matrix and particle distributions.

Anders E. W. Jarfors
Jönköping University, School of Engineering, Department of Materials and Manufacturing, Box 1026, 55111 Jönköping, Sweden

Rohollah Ghasemi
Husqvarna AB, Drottninggatan 2, 561 82 Huskvarna, Sweden

Samuel Awe
Automotive Components Floby AB, Aspenäsgatan 2, 521 51 Floby, Sweden

Chaitanya Krishna Jammula
Jönköping University, School of Engineering, Department of Materials and Manufacturing, Box 1026, 55111 Jönköping, Sweden

Tab.1 - Composition of the materials investigated.

Materials	Si	Fe	Mg	Ti	Al	SiCp
L15	2.94	1.09	0.51	0.04	81.36	15
L20	1.82	1.23	0.57	0.025	76.17	20
S15	2.38	1.11	0.54	0.04	81.31	15
S20	1.94	1.32	0.58	0.023	76.07	20

EXPERIMENTAL

Materials and Casting

The Al-MMC material was cast using conventional high pressure die casting and through rheocasting. In rheocasting, the RheoMetal™ process was used to prepare the slurry, with the so-called enthalpy exchange material made from the same material as in the melt. In the rheocasting process, the same high pressure die casting set-up was used to cast the slurry. Spectrometer and EDS analysis are used to get information about the chemical composition of the material. The chemical composition of the material is shown in table 1. It should here be noted that the resulting composition of the L15 and S15 material is that the matrix has a slightly higher Si-content as compared to the L20 and L20 samples that are richer in SiC.

Microstructural analysis

An Olympus GX microscope was to study the microstructure. For the quantitative analysis t. Quantitative particle characteristics analysis was made using the Olympus stream image analysis software. To better reveal the microstructure; the composite material was etched using a 10% NaOH and distilled water solution.

Hardness and wear testing

Hardness Test: Hardness was measured using the Rockwell C and Micro-Vickers hardness test. The Rockwell C test was carried out at room temperature, with a 50 kgf load with a dwell time of 10-15 seconds at six different locations per sample. Rockwell hardness was converted into Brinell harness for comparison taking into consideration the maximum value of 800 BHN. The Micro-Vickers hardness test was carried out at room temperature with 100gms load with a dwell time of 10-15 seconds.

Micro-Scratch Test: Micro-scratch test was carried out on Nano vantage test machine with a depth sensor. Three micro-scratches were made under progressive load, increasing from 5 mN to 1000 mN with a length of 1000μm. The scratch test was made according to ISO 14577- 1:2002, at 25°C. A sphero-conical shaped diamond tip with a cone angle 2θ=90o was used. (4)

Dry Sliding Wear Test: Reciprocating sliding wear test using a pin on plate test under dry conditions, suitable for brake discs, especially for holding brakes was made. (5) The pin samples were flat-ended with 8mm diameter and 20mm length. Pins are made from all materials. The substrate was made from the L20 material (50mm length, 20mm width and 15mm thick). The test load was 20N measured using a load cell. Both normal force and friction force was measured to evaluate the coefficient of friction (CoF). For each material, five pins were tested up to 120mins. The pin wear was measured base on weight change with an accuracy of 0.0001 g. Each sample was cleaned ultrasonically in acetone and dried before measurement. All tests were carried out at room temperature. The worn surfaces of the pins were examined under Scanning Electron Microscope, (SEM).

RESULTS AND DISCUSSION

Microstructure

The microstructure is shown in Fig. 1. The particle number density is clearly higher for the 20% SiC additions as compared to the 15% additions. It is also visible that for the semisolid cast samples, coarser light α-Al regions are visible (S15 and S20), not visible in the conventionally cast samples (L15 and L20).

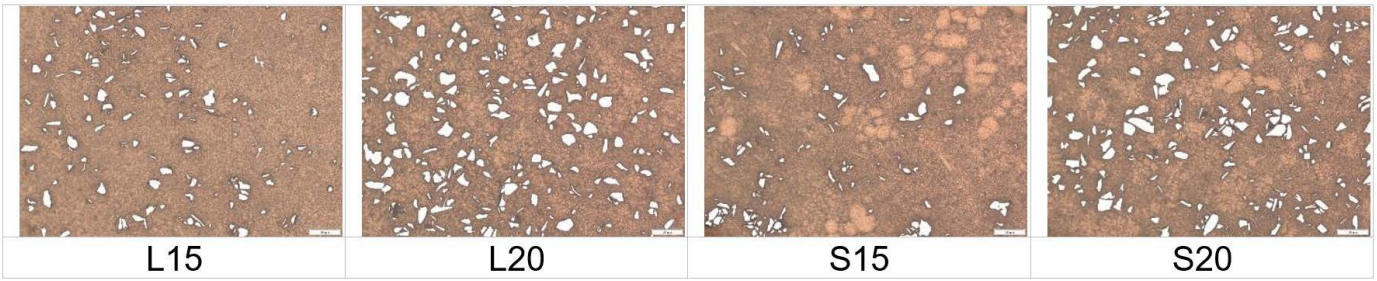

Fig.1 - Illustration of the microstructures with L15 and L20 samples being cast using conventional high-pressure die casting and S15 and S20 being cast using rheocasting. Scale bar is 100μm.

The nearest neighbour distances vary primarily between the 15 and 20% SiC additions and there are no significant differences in the average distance between the S15 and L15 and the S20 and L20, Fig. 2a). This suggests that the differences should be due to the additional level (15 or 20 % SiC) and not between the casting methods (S or L samples). The distribution of nearest neighbour distances, Fig. 2b shows that the distribution differences between S20 and L20 are nearly none, and only the L15 and S15 samples show differences. L15 shows a more even distribution compared to L20 and S20. Comparing S15 to L15, S15 has a broader distribution, especially with a higher contribution from large nearest neighbour distances. S15 also har a higher fraction in the range below 10μm.

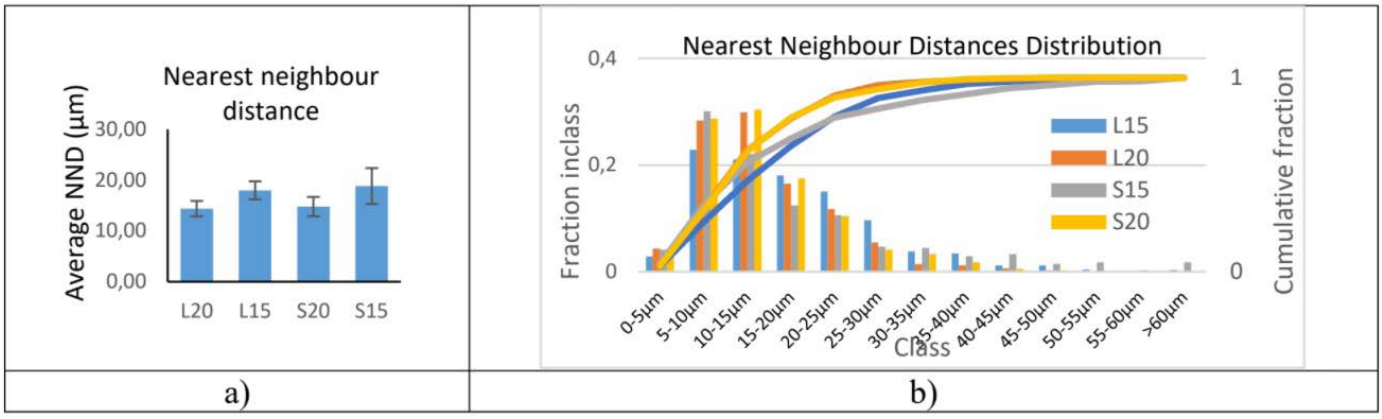

Fig.2 - Nearest neighbour distances a) averages and error, b) distribution of nearest neighbour distances.

HARDNESS TEST

The Micro-Vickers hardness did not show any significant differences between the different samples, Fig. 3a. The 20%SiC addition resulted in a larger scatter of the data. Rockwell C hardness displayed substantial differences in hardness, decoupled from the SiC particle addition, Fig. 3b. L15 was the hardest, followed by L20 and S20 whilst S15 was the softest, Fig. 3b. The difference between the Micro-Vickers test and the Rockwell C test is that Micro-Vickers is based on intent size and thus depending on the plastic deformation. Rockwell C is based on the difference in displacement depths between two loads and as such is affected by deformation hardening taking place during the indentation. The matrix properties may thus become dominant. The variation suggests that the matrix of the semisolid cast materials is softer than the conventionally cast material. It should particularly be noted that L15 is much harder than S15. Converting the Rockwell C data to Brinell hardness showed the same trend, even though the Brinell scale was capped at 800, Fig. 3c.

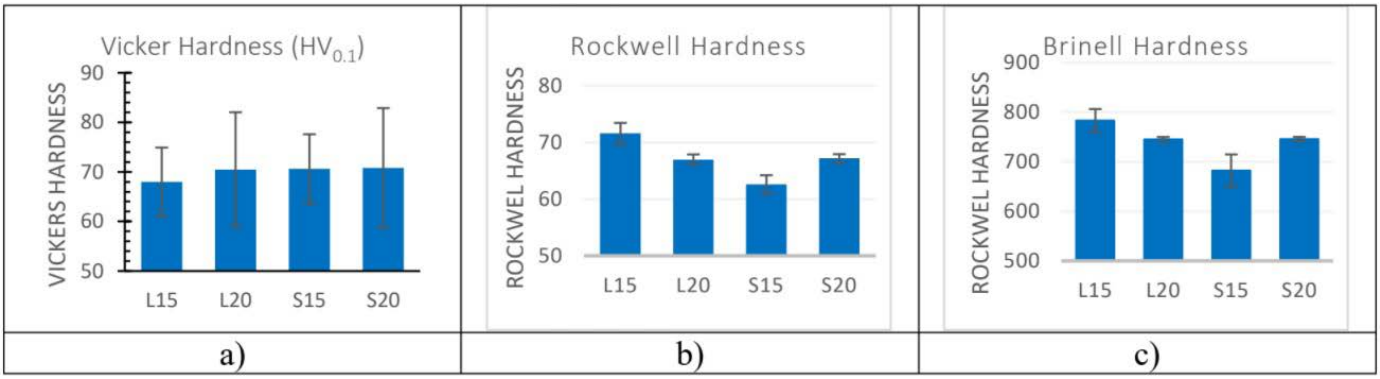

Fig.3 - Hardness of the composite, a) Micro-Vickers results, b) Rockwell C hardness results, c) Brinell hardness converted from Rockwell hardness.

MICRO SCRATCH TEST

In the scratch test, there is a clear difference between the semisolid materials and the conventionally cast materials, Fig. 4. The scratch hardness was an inversely proportional load for the L15 and L20. For the semisolid cast samples, a breakthrough threshold above 200mN for S15 and above 400mN for S20 indicating a possible instability due to limited subsurface strength.

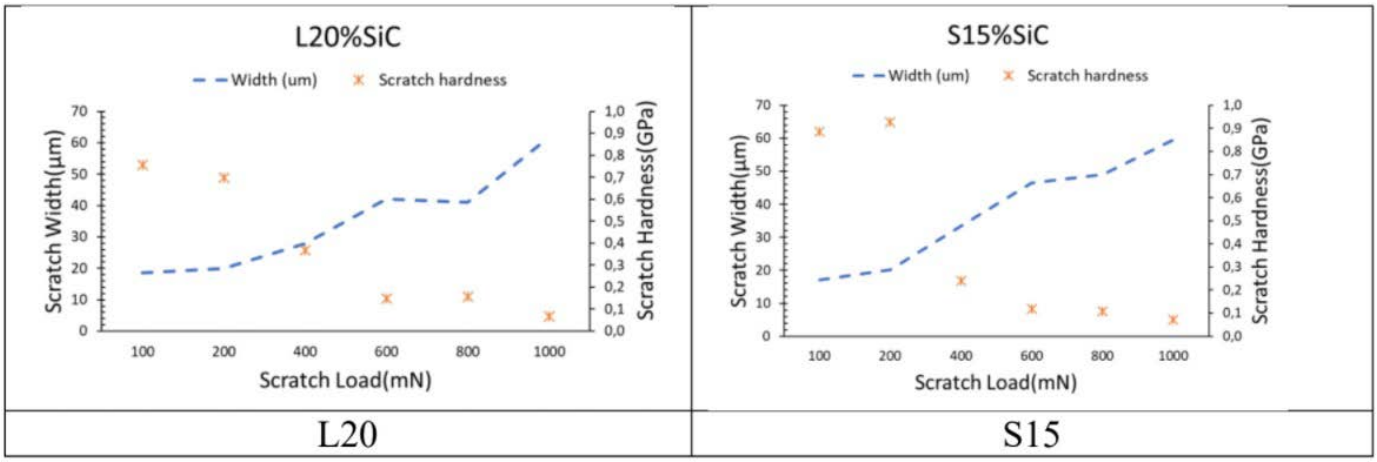

Fig.4 - Scratch test using progressive load.

DRY SLIDING WEAR TEST

Based on the Archard equation (6), the slope under constant load should be linear Eq (1)

$$\Delta m = K\frac{Fvt}{H} \quad \text{Eq. (1)}$$

Where v is average sliding speed (m/s), t is the duration (s), F is load (kgf), H is hardness (Brinell hardness) and K is a material system parameter that depends on the wear and contact mechanisms (adhesive or abrasive wear). Eq (1) implies that increased hardness gives the lower wear rate. Based on the results, Fig. 3c, the material weight loss should be S15>S20>L20>L15. In Fig. 5, the rate of wear loss was S20>L20>L15>S15. A higher SiC addition, (L20 and S20) resulted in a higher wear rate than the lower additions (L15 and S15). Furthermore, the hardest material L15 showed a higher mass loss than the softest material S15. This implies that the material hardness is not dominant but rather the nature of the contact between the surfaces, implicitly included in the coefficient K. (6)

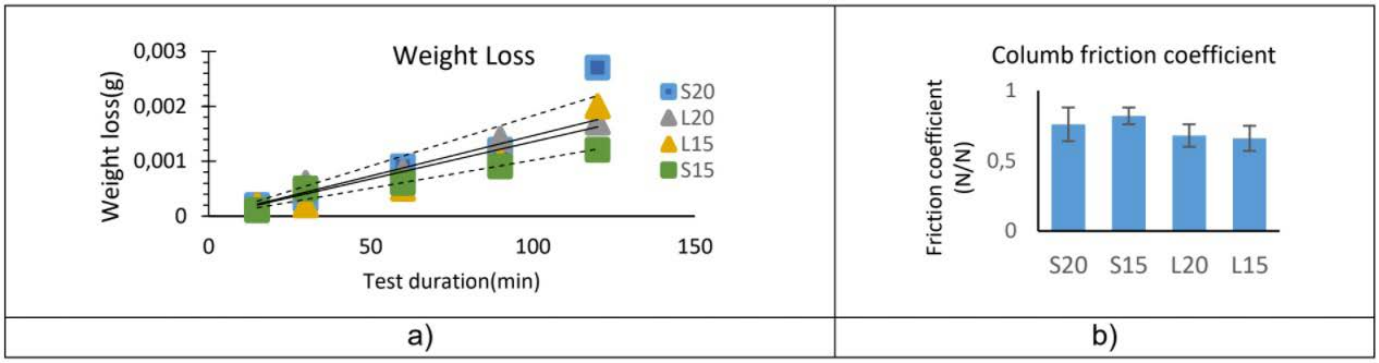

Fig.5 - a) Mass loss from the dry sliding wear test b) CoF during the sliding wear test.

Friction also depends on contact characteristics and measured through the CoF, Fig. 4 b), but an increase in friction cannot explain the difference in wear performance between S15 and S20. Noteworthy is that the hardest material, L15, had the lowest CoF and the material with the lowest wear rate, S15, was the softest, with the highest CoF. The time-series data of the CoF, Fig. 6, shows clear differences between the different materials. Firstly, the average CoF value corresponds to the floor value of CoF under steady-state conditions. Besides, several adhesive wear events generate a CoF above unity. S20 displays the highest number of adhesive events. L15 and S15 show lower amounts of adhesive events, compared to L20 and S20. Adhesive wear performance is thus important for Al-SiCp composites. The worn surfaces showed significant differences, Fig. 7. Both S15 and L15 showed adhesive wear as material smearing with burr formation in L15. This suggests a more abrasive nature of wear in L15, compared to S15. Smearing with loose debris was found in S20 surface. This indicated that tribo-layer was unstable in S20 supported by an increased presence of silicon in EDS analysis compared to S15. The Si originated from exposed SiCp-particles in the surface. L20 showed open pores in the trbolayer with clusters of SiCp-particles visible. L20 showed less debris compared to S20 which suggests that the tribolayer was more stable in L20. Abrasive wear was more predominant in L20 compared to L15 and S15, supporting that the tribolayer was necessary for the wear resistance of Al-SiCp-MMC. The importance of the tribo-layer build-up is also visible in the CoF shown in Fig. 6. The friction coefficient first starts on low but varying values indicating adhesive episodes. Later this is stabilising close to the average values with more adhesive events.

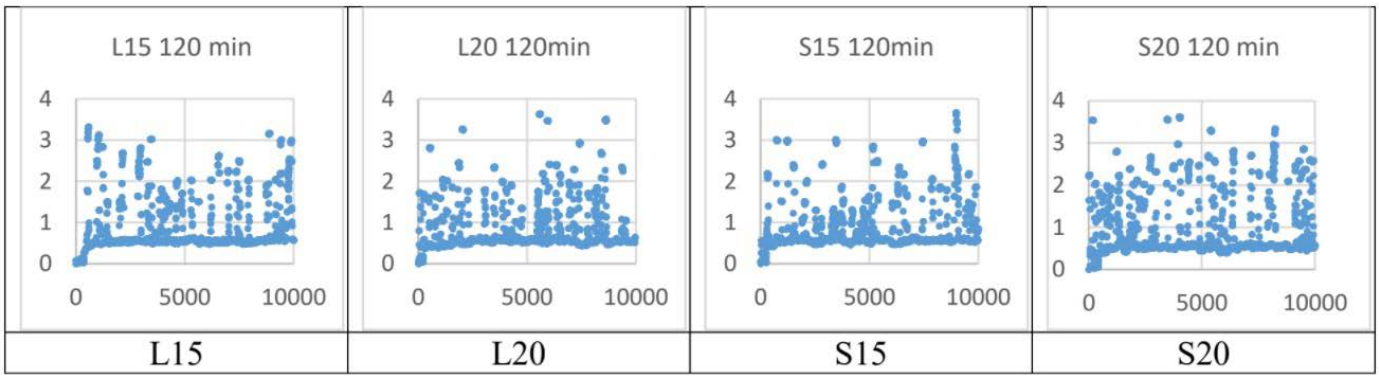

Fig.6 - CoF as a function over time for samples L15, L20, S15 and S20 illustrating the number of adhesive events where the friction force exceeds the normal force.

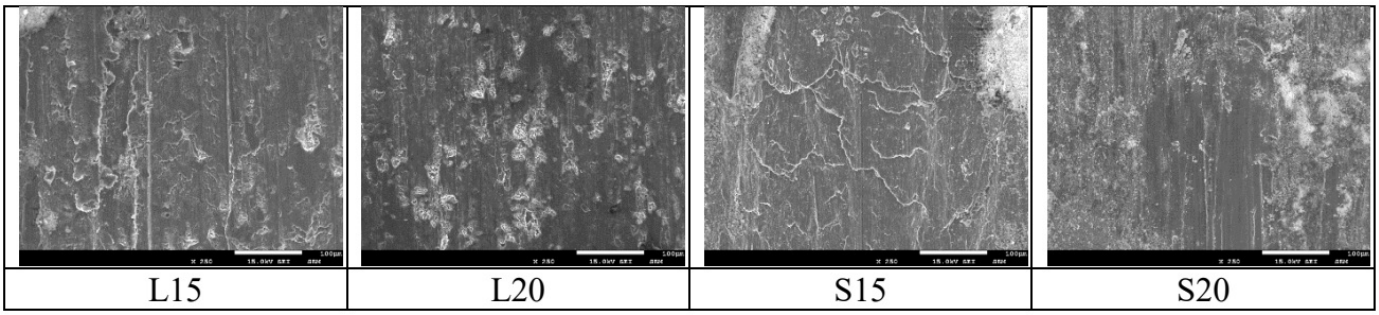

Fig.7 - Wear surface samples L15, L20, S15 and S20 illustrating the adhesive and abrasive nature of the wear mechanisms as well as the stability of the tribo-layer. (Scale bar is 100μm).

CONCLUSIONS

In the current study, the wear performance of conventionally cast Al-SiCp MMCs was studied. It was shown that there is a highly complex interaction between the wear and friction properties of the material. The wear loss as function could not be established clearly as suggested by hardness as suggested by Archard's law. Instead, the nature of the contact has a great influence on the wear, resulting in that the softest material with the highest friction coefficient had the lowest wear.

ACKNOWLEDGEMENTS

The materials supplied by AC Floby, but cast at Jönköping University as part of an MSc project.

REFERENCES

[1] Serrenho AC, Norman JB, Allwood JM. The impact of reducing car weight on global emissions: the future fleet in Great Britain. Philos Trans R Soc A Math Phys Eng Sci [Internet]. 2017;375(2095):20160364. Available from: http://rsta.royalsocietypublishing.org/lookup/doi/10.1098/rsta.2016.0364

[2] Sadagopan P, Natarajan HK, Praveen Kumar J. Study of silicon carbide-reinforced aluminum matrix composite brake rotor for motorcycle application. Int J Adv Manuf Technol. 2018;94(1–4):1461–75.

[3] Sijo MT, Jayadevan KR. Analysis of Stir Cast Aluminium Silicon Carbide Metal Matrix Composite: A Comprehensive Review. Procedia Technol [Internet]. 2016;24:379–85. Available from: http://dx.doi.org/10.1016/j.protcy.2016.05.052

[4] Ghasemi R, Johansson J, Ståhl JE, Jarfors AEW. Load effect on scratch micro-mechanisms of solution strengthened Compacted Graphite Irons. Tribol Int [Internet]. 2019;133(January):182–92. Available from: https://doi.org/10.1016/j.triboint.2019.01.010

[5] Poulios K, Drago N, Klit P, De Chiffre L. A reciprocating pin-on-plate test-rig for studying friction materials for holding brakes. Wear. 2014;311(1–2):40–6.

[6] Popov V. Generalized archard law of wear based on rabinowicz criterion of wear particle formation. Facta Univ Ser Mech Eng. 2019;17(1):39–45.